Nanoscale

Accepted Manuscript

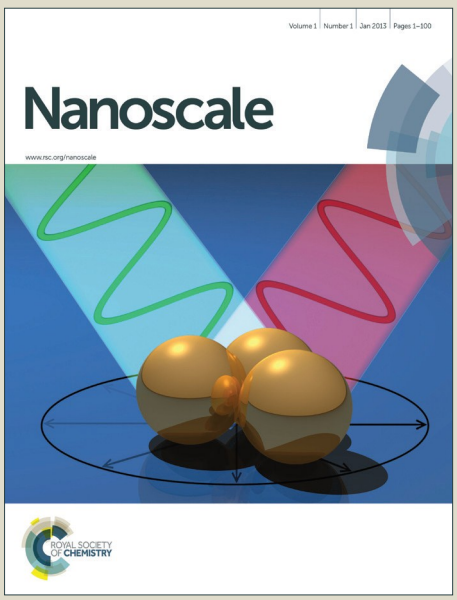

ROYAL SOCIETY OF CHEMISTRY

www.rsc.org/nanoscale

Atomistic simulations of electrochemical metallization cells: mechanisms of ultra-fast resistance switching in nanoscale devices

Nicolas Onofrio, David Guzman, and Alejandro Strachan*

School of Materials Engineering and Birck Nanotechnology Center

Purdue University, West Lafayette, Indiana 47906 USA

We describe a new method that enables reactive molecular dynamics (MD) simulations of electrochemical processes and apply to study electrochemical metallization cells (ECMs). The model, called EChemDID, extends the charge equilibration method to capture the effect of external electrochemical potentials on partial atomic charges and describes its equilibration over connected metallic structures, on-the-fly, during the MD simulation. We use EChemDID to simulate resistance switching in nanoscale ECMs; these devices consist of an electroactive metal separated from an inactive electrode by an insulator and can be reversibly switched to a low-resistance state by the electrochemical formation of a conducting filament between electrodes. Our structures use Cu as the active electrode and SiO_2 dielectric and have dimensions at the foreseen limit of scalability of the technology, with dielectric thickness of approximately 1 nm. We explore the effect of device geometry on switching timescales and find that nanowires with an electroactive shell, where ions migrate towards a smaller inactive electrode core, result in faster switching than planar devices. We observe significant device-to-device variability in switching timescales and intermittent switching for these nanoscale devices. To characterize the evolution in the electronic structure of the dielectric as dissolved metallic ions switch the device, we perform density functional theory calculations on structures obtained from an EChemDID MD simulation. These results confirm the appearance of states around the Fermi energy as a

* Corresponding Author: strachan@purdue.edu

metallic filament bridges the electrodes and show that the metallic ions and not defects in the dielectric contribute to the majority of those states.

1. Introduction

Electrochemical processes are at the heart of a wide range of established and emerging applications from energy storage[1] and materials processing to nanoelectronics[2,3,4,5] and neuromorphic computing.[6,7] In nominally all applications of current interest the operation of devices is an emergent phenomena that originates from the interplay between processes with disparate time and length scales; these include: electrochemical reactions at complex interfaces, dissolution and deposition of ions, their transport and aggregation, injection and trapping of electrons and holes, changes in composition, phase and valence change in the electrolytes, Joule heating and electromigration. Remarkably, some of these devices can be scaled down to the nanoscale and operate at nanosecond timescales,[8] opening exciting potential applications but also complicating their experimental characterization. As a result, the atomistic mechanisms that govern the operation of devices like batteries, pseudocapacitors and electrochemical metallization cells are not fully understood. Given these significant challenges and the increasingly important role of molecular dynamics simulations in materials science, it is perhaps surprising that the first attempts to describe electrochemical processes using empirical force field methods date back only a few years.[9,10,11] In this paper we describe the electrochemistry dynamics with implicit degrees of freedom EChemDID method, that enabled the first fully atomistic simulations of electrochemical metallization cells (ECMs) that can exhibit

ultra-fast resistance switching and apply to explore the role of device geometry and atomic processes in the switching of ECMs.

Nanoscale resistance switching electrochemical devices hold great promise as memory and logic elements in future nanoelectronics devices with the potential to contribute to the extension of Moore's law beyond the rapidly approaching *end of scaling* and even enable neuromorphic computing. *Resistance-* and *threshold-switching* electrochemical cells are fascinating devices that can reversibly or irreversibly change their electrical resistance with an applied voltage via a variety of processes induced by electrochemistry.[12,13,14] Their deceptively simple structure, consisting of two metallic electrodes separated by a solid dielectric or electrolyte, seems at odds with the wide range of I-V characteristics that can be achieved by the appropriate choice of materials:[13] from linear to non-linear bipolar and nonpolar resistance switching to threshold switching (an abrupt but reversible change in resistance). Importantly both from applied and basic science points of view, these devices can exhibit switching in nanosecond timescales[8] and scaling to approximately ten nanometers,[15] where the distinction between material and device becomes meaningless. Despite the significant experimental and theoretical efforts devoted to these devices in recent years the underlying materials processes responsible for their remarkable properties are not fully known. Even the switching mechanisms, interfacial reactions, and the nature of the conducting paths are not known in many cases.[13] Recent experimental studies based on high-resolution transmission electron microscopy imaging[16] and scanning tunneling microscopy[17,18] are providing key insight and quantitative information regarding the fundamental physics of these devices. However, these techniques are not without limitations, especially when dealing with devices at their

miniaturization limit (few nanometers) and operating at ultra-fast speeds (nanoseconds). In Section 3 of this paper we use EChemDID to explore the resistive switching of nanoscale ECMs consisting of Cu as the active electrode and SiO_2 dielectrics. We focus on the effect of device geometry on switching dynamics and find that nanowire geometry tends to facilitate the creation of metallic filament. Interestingly, the simulations show that switching occurs with negligible changes in the atomic structure of the amorphous dielectric. Section 4 introduces multiscale simulations coupling EChemDID to ab initio electronic structure calculations to study the electrical characteristics of the systems. We find an increased number of states around the Fermi energy of the dielectric as a metallic filament bridges the electrodes and that these states are predominantly originate on the metallic ions and not on defects in the dielectric.

2. Reactive molecular dynamics of electrochemistry

2.1 Reactive MD simulations

The use of many-body, partial bond-orders to describe covalent interactions[19,20] together with charge equilibration methods (QEq, initially proposed by Rappe and Goddard[21] and by Mortier at al.[22]) to obtain geometry dependent partial atomic charges led to the development of powerful reactive force field such as ReaxFF,[23] COMB[24] and REBO[25]. These reactive potentials enable large-scale (multi-million atoms) molecular dynamics of materials processes involving chemistry. Examples of recent successes include areas as disparate as shock-induced decomposition of explosives,[26] combustion,[27] water reactions in cement,[28] and reactions in nanomaterials.[29] In this paper we use the reactive force field ReaxFF that has been parameterized to describe Cu, SiO_2 and its interactions[30,31] to model the ECMs of interest. A detailed description of the potential including extensive validation tests and sensitivity analysis

are included in the Supporting Information of Ref. [10] and will not be repeated here. The following subsection describes how EChemDID enhances reactive MD simulations enabling the description of an external electrochemical potentials to reactive metallic electrodes.

2.2 EChemDID simulations

Over the last 10 years Strachan and collaborators developed a family of simulation techniques denoted dynamics with implicit degrees of freedom (DID)[32] that was recently extended to describe electrochemistry. DID couples particle dynamics with the evolution of degrees of freedom that are not captured explicitly in the particle description. For example, an important application of DID is the capability of describing the thermal role of electrons in MD simulations of metals via an implementation of the two-temperature model. [33]

DID describes time evolution of the local electronic temperature in the vicinity of atom *i* (T_i^{ele}) using the atoms as a grid and coupling to the atomistic dynamics via the position update equation:[33]

$$\dot{R}_i = V_i + \gamma_i F_i \tag{1a}$$

$$\dot{V}_i = \frac{F_i}{M_i} \tag{1b}$$

$$\dot{E}_i^{ele} = C_i \dot{T}_i^{ele} = \gamma |F_i|^2 + \kappa^{ele} \nabla^2 T_i^{ele} \tag{1c}$$

where the subscripts denote atoms, *R,V, F* and *M* are atomic position, velocity, force and mass, and κ^{ele} is the thermal conductivity of the valence electrons. The dynamical parameter γ_i governs the strength and directionality of the energy transfer between the electronic and atomic subsystems at location *i*. It is defined as: $\gamma_i \propto \mu\left(T_i^{ion} - T_i^{ele}\right)$ where T_i^{ion} is the local

atomic temperature in the vicinity of atom *i* and μ is the strength of the electron-phonon coupling. The Laplacian in equation (1c) is solved numerically via:[32,33]

$$\nabla^2 T_i^{ele} = \sum_{j \neq i} \frac{T^i - T^j}{R_{ij}^2} \omega\left(R_{ij}\right) \quad (2)$$

where ω is a localized weighting function that defines the extent of the local neighborhood of the calculation; see Ref. [32] and its supplementary information document. The range of this local weighting function is a few atomic distances and its details do not affect the results in an appreciable manner; this is due to the fact that in the applications of interest the local electronic temperature and its Laplacian do not vary significantly within atomic distances. The DID formulation has several desirable properties, total energy (ions plus electrons) is conserved, the equations are Galilean invariant and we demonstrated the strong foundations of the approach in statistical mechanics.[33] The method was recently extended to accurately describe metal/semiconductor and metal/insulator interfaces by enabling direct electron-phonon coupling across the interface.[34]

We recently combined the DID method with a modified version of charge equilibration to enable the application of external voltages in reactive MD simulations. This new method, called EChemDID, enabled the first atomistic simulation of an electrochemical metallization cell.[10] In the QEq formalism, partial atomic charges are computed on the fly during molecular dynamics simulations from a self-consistent minimization of the total electrostatic energy, written as:[21,22]

$$E(\{R_i\}\{Q_i\}) = \sum_i^N \left(\chi_i Q_i + \frac{1}{2} H_i Q_i^2\right) + \sum_{i<j}^N Q_i Q_j J\left(R_{ij}\right) \quad (3)$$

where J(R) is the distance dependence of the electrostatic interaction (often shielded Coulomb). QEq requires atomic electronegativity χ_i and hardness H_i parameters as input and is often parameterized against partial charges obtained from *ab initio*. The application of an external electrochemical potential difference $\Delta\phi$ between atoms in two electrodes causes an energy difference in an electron of $e\Delta\phi$; this can be accomplished within QEq by changing the electronegativity in one electrode to $\chi_i \rightarrow \chi_i + \Delta\phi/2$ and to $\chi_i \rightarrow \chi_i - \Delta\phi/2$ in the other. To simulate the effect of an external electrochemical potential EChemDID assigns an additional dynamical variable to each metallic atom to represent the local external electrochemical potential ϕ_i. This value is added to the atomic electronegativity used for charge equilibration, thus affecting the charge distribution and enabling electrochemical processes.

The challenge is to dynamically equilibrate the electrochemical potential in connected metallic regions during a reactive simulation, including atoms dissolving into the dielectric or depositing from it. EChemDID describes this equilibration process using a diffusion equation for ϕ_i:

$$\dot{\phi}_i = k^{\phi}\nabla^2\phi_i, \qquad (4)$$

where k^{ϕ} is an effective diffusivity for the electrochemical potential. This fictitious dynamics (instead of solving Maxwell's equations) is chosen for computational convenience. The electrochemical potential propagates at the speed of light and, consequently, its equilibration occurs much faster than any atomistic processes. For our purposes the details of this ultra-fast equilibration are irrelevant and sufficiently fast diffusive equilibration meets our needs. We numerically solve equation (4) on-the-fly during the MD simulation using atoms as a grid and a local weighting function as in the DID method described above, Eq. (3).

Figure 1 exemplifies EChemDID in the two devices of interest in this paper: i) a configuration with a fin-shaped active electrode and ii) a core/shell nanowire. The snapshots show the metallic atoms in the systems (the dielectric is not shown for clarity) and atoms are colored by electrochemical potential in the top panels and partial atomic charge in the bottom ones. In these simulations an electrochemical potential difference of 8V is applied to a group of atoms in the active (electropositive, blue) and inactive (negative, red) electrodes far away from the electro-active interfaces. As seen in the top panels, EChemDID equilibrates the applied electrochemical throughout the metallic structures and affects the atomic charges, bottom panels. We see that charges appropriately localize at the free surface of the metallic structures.

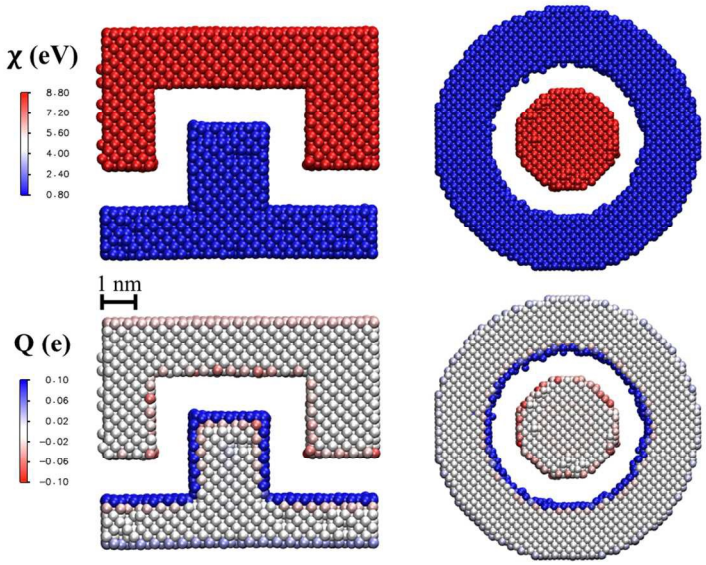

Figure 1. Atomic structure of the ECM devices studied and the equilibrated local electrochemical potential under an applied voltage of 8 V (top) as well as the corresponding partial atomic charges (bottom)

An important by-product of EChemDID is its ability to describe resistive electron transport when a metallic filament bridges between two electrodes kept at different potentials. This originates

from the diffusive nature of Eq. (4) used to equilibrate the electrochemical potential. We note that under diffusive electrical transport the gradient of the electrochemical potential is proportional to the electronic current density; thus, the Laplacian in the RHS of Eq. (4) represents the divergence of the current density around site *i* (i.e. time derivative of the total charge density around the site). The details of the calculation of an electronic current are explained in Ref.[11] and will not be repeated here in the interest of brevity. EChemDID has been implemented in the parallel molecular dynamics package LAMMPS from Sandia National Laboratories[35] and is available for download from our website.[36]

EChemDID summary. In concluding this section, we point out that simulations presented here involve no tunable parameters and are, thus, predictive. The inputs are force field parameters that were obtained from ab initio simulations designed to describe the various interactions but not specifically designed for electrochemistry or ECM simulations. The EChemDID parameters to describe the equilibration of electrochemical potential have a negligible role in the simulations are only chosen so that the equilibration of the voltage occurs fast compared with atomic processes. We also highlight that simulations of this complexity necessarily involve approximations, neglect processes and include uncertainties. These include the use of a force field to describe atomic interactions, limitations intrinsic to the charge equilibration method used, and the neglect of electronic transport when a conducting filament forms. As discussed in Section 5 we believe these approximations do not affect the main results of our simulations.

As with all other simulation techniques EChemDID is not without approximations. In addition to the use of an interatomic potential to describe interactions, EChemDID does not describe electron transport (including trapping defects). Consequently, Joule heating and electron

migration are not modeled at this point. These processes would not play an important role until a bridging filament is formed, enabling electronic current. However, a compliance current is imposed to limit electron flow and control the conductivity of the filament;[37,38] thus limiting Joule heating. A characteristic time for thermal equilibration can be estimated as the ratio between a characteristic length squared (taking into account the oxide thickness we can take this as ~4 nm^2) and the thermal diffusivity (a typical value for oxides is 10^{-6} m^2/s). This yields 4 ps, indicating that thermal equilibration occurs in timescales significantly shorter as compared with switching and justify our neglect of Joule heating and the use of a thermostat to maintain constant temperature throughout the simulations. The neglect of Joule heating in the current version of EChemDID implies that RESET is governed by electrochemical dissolution and not aided or driven by Joule heating. This is consistent with experimental observations in bi-polar devices where erase voltages are lower than those required to significant Joule heating[39] but would not apply to unipolar devices.[3]

2.3 DFT electronic structure calculations

Ab initio electronic structure calculations of the operation of the ECMs of interest here will be computationally prohibitively expensive for the foreseeable future; yet, only such calculations can provide answers to some of the key open questions in the field such as the nature of electronic transport. To bridge this gap, we performed EChemDID MD simulations on small simulation cells (275 atoms) and extracted a series of atomistic configurations to study their electronic structure using density functional (DFT) calculations.

The geometry optimization and electronic structure calculations were carried out with DFT using the Vienna *ab initio* simulation package (VASP)[40,41]. Projector-augmented-wave (PAW)

pseudopotentials[42] were used to describe core electrons, and the electron exchange-correlation potential was computed within the generalized gradient approximation (GGA) as proposed by *Perdew-Burke-ErnZerhof* (PBE)[43]. The kinetic energy cutoff was set to 500 eV and only gamma-point calculations were carried out due to the relatively large simulation cells. The conjugate gradient method was used for the structural relaxation with a maximum force tolerance of 0.01 eV/Å and the self-consistent field electronic relaxation proceeds until a tolerance of $1x10^{-5}$ eV is reached.

3. ECM simulations: role of dielectric chemistry and structure on switching

3.1 Systems of interest and simulation details

We study ECM cells with Cu as the active electrode and amorphous SiO_2 electrolytes; this system is attractive due to the wide availability of experimental data and compatibility with CMOS processing. In order to study the effect of device geometry on switching timescales and filament stability, we focus on three classes of devices, see Figure 2: i) a parallel electrodes setup with an active electrode patterned in a conical shape, as described in our previous study,[10] ii) a nanowire geometry with a shell made of the active electrode and an inactive electrode core separated by the dielectric (center panels of Figure 2), and iii) a structure with a fin shaped active electrode (right panels in Figure 2). We impose periodic boundary conditions in two dimensions for the parallel electrodes and fin devices and 1D periodic boundary conditions in the nanowires. For better statistics, we generated an ensemble of structures of each type of devices differing only in the atomic structure of the amorphous dielectric; these

will be denoted C1-C4 (conical electrode), NW1-NW4 (core-shell nanowires) and F1-F4 (for the fins). In order to isolate the effect of device geometry on switching timescales, the nanowire and fin devices both have dielectric thicknesses of 1 nm; this is also the separation between the tip of the cone and the inactive electrode in the parallel plates device. In this way, the distance ions need to migrate to reach the inactive is nominally identical in all cases. For simplicity, the inactive electrode is modeled using Cu interatomic potential but all atoms are kept at fixed positions throughout the simulation.

The number of atoms in the devices range from 20,594 to 47,847 and the MD simulations of switching involve up to 2.5 ns timescales. Such system sizes and timescales are beyond the capabilities of ab initio simulations today and in the near future, highlighting the importance of empirical approaches like EChemDID and reactive force fields. Even with EChemDID/ReaxFF, the simulations presented here are computationally intensive; for example, a 1.5 nanosecond simulation of the NW1 device takes 670 hours of wall clock time running on 32 cores of Purdue University's Conte compute cluster.

Figure 2. Geometry of the three types of ECM cells studied: parallel electrodes with patterned active electrode, core/shell nanowires, and fin active electrodes. Top panels show relaxed geometries and bottom show open representations of the structures.

Generating well-relaxed amorphous structures for the dielectric is critical for the reliability and reproducibility of the simulations. We start from an amorphous SiO_2 (a-SiO_2) system with 30,000 atoms generated following a melt and quench procedure as described in our previous work.[45] The a-SiO_2 is then patterned in the desired shape and inserted between the active and inactive electrodes. Additional Si and O atoms are added to the electrolyte in order to maintain the overall stoichiometry of as SiO_2. The dielectric is then re-annealed in the presence of the electrodes; we heat the SiO_2 to T=4000 K and maintain this temperature for 50 ps while keeping

the atoms in the electrodes as a rigid body. We follow this high-temperature relaxation by an annealing to T=300 K in 370 ps (cooling down at 10 K/ps). The last step in the preparation of the cells for electrochemical switching is thermalization of the entire system (including electrodes) at a temperature of 300 K. The final cells are stress free and the densities of the a-SiO_2 dielectric are consistent with previous work and in good agreement with experiment.

All simulations are performed using the parallel MD simulator LAMMPS[35] with atomic interactions described using ReaxFF as described in Ref.10. All simulations use the following EChemDID parameters. The range of the weighting function that describes the equilibration of the electrochemical potential is set to 4Å and the parameter k^{ϕ} that describes the fictitious electrochemical diffusivity is 4 $Å^2$/fs.

3.2 Reactive MD simulations of switching

Before operation, i.e. the periodic switching of the device to the low-resistance state (SET) and the high-resistance state (RESET) the devices need to be *FORMED,* i.e. switched for the first time. This initial switching often requires higher voltages and longer times than the subsequent SET processes. In order to simulate the FORMING of the devices described in Section 3.1 we apply an electrochemical potential of 8 V across the cell, setting the electrochemical potential of +4 V to the active electrode and -4 V to the inactive one. The electrochemical potential is externally set for a metallic group of atoms away from the electrochemically active interfaces and EChemDID equilibrates the potential across the two metallic electrodes, see Figure 1.

The top panels of Figure 3 show the EChemDID current (see Eq. 10 in Ref. 11) between the electrodes as a function of time during the FORM simulations. A non-zero value indicates the

presence of the bridging metallic filament between the active and inactive electrode. The results are consistent with our previous simulations on parallel electrode setups with patterned active electrodes.[11] These simulations showed switching timescales ranging from approximately 0.5 ns to 5 ns and intermittent switching in many cases caused by metastable single-atomic chain filaments. These switching timescales are consistent with experimental results[5]; we consider this agreement quite remarkable given that none of the model parameters where tuned to describe neither ECM cells nor electrochemical reactions.

Interestingly, the simulations reported in Figure 3 show that the nanowire devices tend to switch at shorter times than the FIN ones. Devices NW3 and NW2 switch within ~0.5 and ~1.2 ns of the application of the voltage while no FIN device switches before 1.7 ns. Devices NW4 and NW1 exhibit intermittent switching before 1.5 ns (denoted by a weak and fluctuating current). We found that the NWs switching timescales are consistent with the geometries studied in Ref. [10] composed of conical and triangular patterned active electrodes. As the Cu ions dissolve into the dielectric and move towards the inactive electrode core, their density increases and so does the chance of forming nanoscale Cu clusters that are critical for switching. Figure 3 (bottom panels) shows the time evolution of the density of Cu atoms dissolved in the dielectric. The density of Cu ions in the dielectric increases faster in the NW devices. The EChemDID currents and Cu concentration in Figure 3 indicate that reaching a threshold density of Cu dissolved in the dielectric is a necessary condition for stable switching but it is not sufficient. Consistent with Ref. [10], our results indicate that stable switching requires at least 4% Cu per SiO_2 atoms but that this alone does not guarantee stable switching. We attribute the slower switching timescales of the FIN devices to the large fraction of their

electrode/dielectric interface being atomically flat (perfectly flat interfaces tend to slow the copper dissolution and therefore increase switching time, as will be discussed in Section 4). In addition, the nanowire geometry leads to a convergence of the dissolved ions into smaller areas as they approach the inactive core electrode favoring the formation of Cu clusters and a conductive filament.

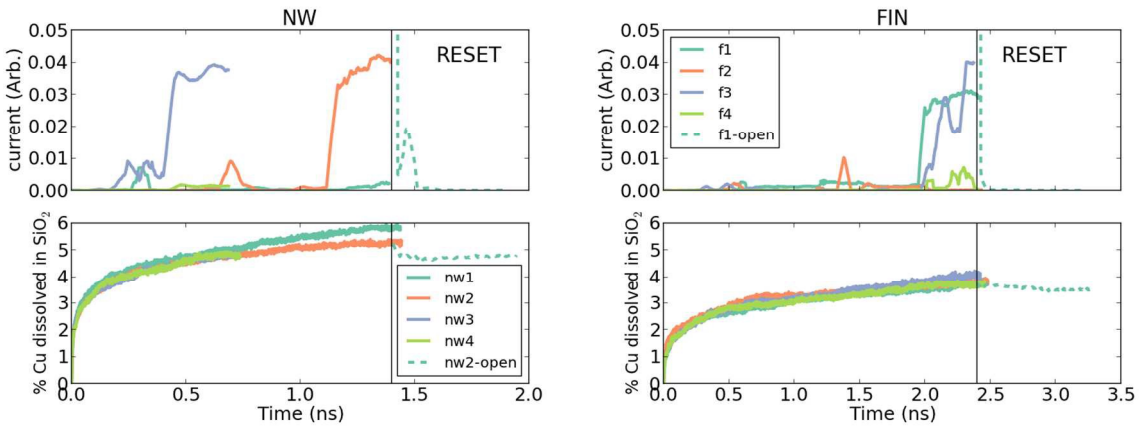

Figure 3. Electrical current computed with EChemDID (top) for nanowire (left) and fin shaped (right) structures as well as the corresponding concentration of Cu dissolved in the solid electrolyte (bottom).

Following the FORMING simulations, we RESET one device of each geometry (NW2 and F1) by reversing the voltage. The results are shown as dotted lines in Figure 3. When the voltage is reversed, a large amount of current is detected because the electrochemical potential has to be re-equilibrated in both electrodes, hence the peaks at 1.5 ns and 2.5 ns observed for the NW2 and F1 structures, respectively. Device F1 switches OFF in a short period of time (in approximately 10 ps) whereas it takes an order of magnitude longer time to switch OFF the NW device (~100 ps). This last observation correlates with the high concentration of Cu dissolved in

the electrolyte for the NW case, slowing down the RESET process. As with FORMING, we expect significant device-to-device variability and study involving several structures and multiple SET/RESET cycles will be required to draw more rigorous conclusions.

3.3 Atomic structure of bridging filaments and dielectric structure

We now focus on the atomistic structure of the nanoscale filaments responsible for the low-resistance state of the devices and the effect of the metallic ions have on the amorphous dielectrics. Knowledge of the shape of the bridging filament is important to predict its electrical characteristics and can provide insight into the process of their formation as well as stability. Similarly important is to understand the processes that occur in the dielectric as it accommodates the ions during switching. For example, it has been postulated that nanoscale voids or cavities created during the FORMING process contribute to subsequent switching steps[44].

Figure 4 shows snapshots of the bridging filaments of the various devices. For clarity only metallic atoms are shown and they are colored according to their partial charges (blue represents positive charge and red negative). The snapshots clearly show the positive charge of the metallic atoms on the surface of the active electrode and ions dissolved into the dielectric. In addition, inspection of atoms that have come into contact with the inactive electrode reveals their electrochemical reduction as described by EChemDID. This chemical reduction stabilizes the atoms in contact with the negative electrode (electro-positive ions in contact with the active electrode are favored to dissolve into the dielectric while dissolution is unfavorable for neutral or negatively charged Cu atoms). As we found for planar geometries, stable switching requires filaments a few atoms thick near the active (positive) electrode but chemical reduction

enables thinner (even single atom) shapes near the inactive electrode. This leads to filaments with approximately conical shapes, thicker near the active electrode. We stress that this shape has its origin in the relative stability of Cu near either electrode and not in the growth process.

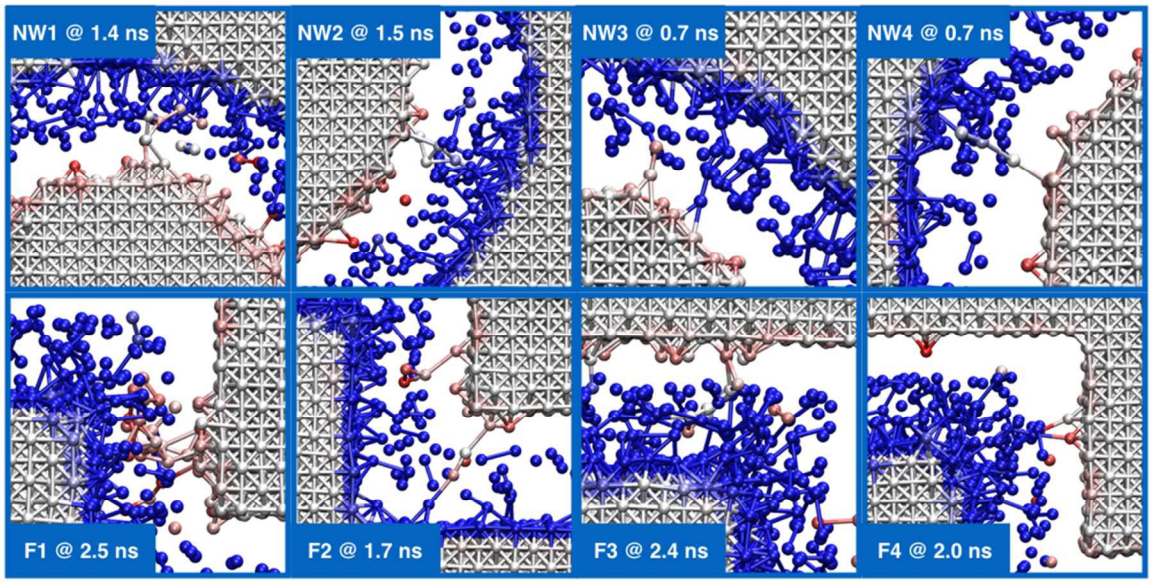

Figure 4. Snapshots of the metallic filaments observed in the simulations. The top and bottom snapshots show filaments observed in NWs and FIN geometries, respectively. The colors represent partial atomic charges ranging from -0.2e (red) to +0.2e (blue) and the amorphous silica has been hidden for clarity.

We now turn our attention to the atomistic structure of the dielectric during switching. Specifically, we focus on possible defects generated as Cu ions migrate through the amorphous structure. A perfect amorphous SiO_2 network consists of SiO_4 tetrahedra bridged by shared O atoms and deviations from this coordination indicate point defects. Thus, we characterize the local coordination of each Si and O atom in the dielectrics during switching and identify defects as sites that deviate from the perfect network (i.e. Si with coordination other that four O atoms and O atoms with coordination other than two Si). Figure 5 shows the temporal evolution of the

fraction of defective atoms in the simulations. As in all amorphous structures a level of intrinsic defects is present from the outset.[45] The small device to device variability denotes the reproducibility of the structure generation procedure and that of the simulation results in general. Quite surprisingly, the density of defects does not increase during the FORMING process, the amorphous structure is able to accommodate the electrochemically dissolved metallic ions. This is an important result and it indicates that the process of FORMING does not generate permanent defects or channels that could subsequently be used for switching during SET and RESET. In addition, this result indicates that structural changes or defects in the dielectric are not likely to contribute to the electronic transport. This observation applies to the nanoscale devices studied here and it is possible that nanoscale pores or channels form in larger devices.

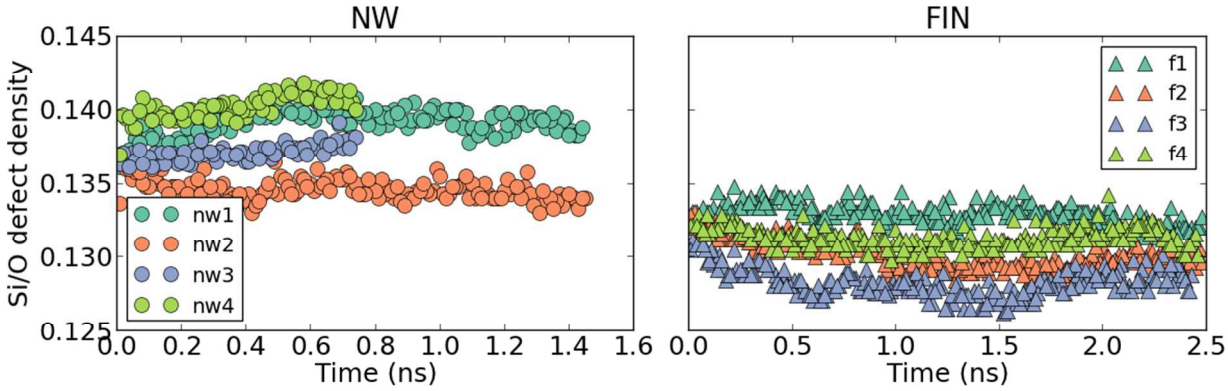

Figure 5. Total point defect density (Silicon and Oxygen) in the a-SiO_2 electrolyte for various ECM cells (left: NWs and right: FIN geometries) as a function of switching time.

4. Multiscale modeling of electronic structure during switching

4.1 Systems of interest and simulation details

In order to characterize the electronic structure of the electrochemical metallization cells during switching we performed DFT calculations of atomic configurations obtained during the switching of a small device as described in Section 2.3. The device, see snapshots in Figure 6 consists of parallel, flat electrodes and a 1.3 nm thick dielectric. The cross-sectional area of the simulation cell is 1.05 x 1.05 nm. The generation of the atomistic structure of the smaller devices only differs from the one laid down in Section 3.1 in the selection of electrodes termination and switching voltage. Due to the limited number of atoms, we use atomistically flat terminations for the electrochemically active and inactive electrodes which makes the initial dissolution of ions into the dielectric more difficult. As in Section 3, the switching process is driven by a potential difference of 8 V across the device.

The total MD simulation time of the small device is 8.25 ns, and copper ions dissolution is initially observed to take place around 3.5 ns. The insets in Figure 6 show the atomic snapshots of the metal-insulator-metal device at different stages of the switching process and these select structures are used for the DFT calculations. The MD generated structures are fully relaxed with DFT-GGA using the settings and tolerances discussed in Section 2.3. The electronic density of states (Kohn-Sham eigenvalues) of the relaxed structure is calculated and projected on the atomic sites of the dielectric region to study how the addition of Cu ions changes its electronic structure.

4.2 Electronic structure evolution during switching

Figure 6 shows the electronic density of states of the dielectric region (amorphous silicon dioxide and dissolved Cu ions) at several stages of the switching process. We observe a relatively small availability of states in the vicinity of the Fermi level (located at zero in all cases) during the first 3.5 ns of the simulation when no copper ions have been dissolved. In these plots, the valence band edge is right below zero and the conduction band starts at near 4eV. As expected, intrinsic defects lead to electronic states within the band gap and we attribute the slight variation in the density of states before any copper is embedded in the electrolyte to variations in the amorphous structure.[46] A detailed analysis of the electronic structure of the initial amorphous SiO_2 including the effect of defects and surface states is beyond the scope of this paper where we focus on the effects on the dissolution of Cu. The dissolution of the first ion takes place at approximately 3.7 ns and this is followed by the rapid dissolution of several nearby ions and the formation of an ultra-thin filament, see snapshots at 3.75 and 4.0 ns. The presence of these metallic ions leads to a sharp increase in the density of states of the dielectric region around the Fermi energy. Further analysis of the density of states via a projection on Si and O atoms (shown as green lines in the bottom panels or Fig. 6) indicates that their contribution to the states around the Fermi energy is minimal. Thus, the electronic states responsible for electronic transport are contributed by the metallic ions and not by defects induced in the dielectric. This is in agreement with other DFT calculations[47] on crystalline silicon dioxide with copper inclusions where copper derived states show a dominant contribution to the top of the valence band and bottom of the conduction band. Pandey *et. al.* reports an increase in the number of localized states in the mid-gap with increasing concentration of

copper and complete metallization for concentrations greater than 3.3×10^{22}cm^{-3}. Our simulations at 4 ns have a Cu concentration of 2.0×10^{22} cm^{-3}. It is also worth noting that the geometric shape of the copper clusters in the amorphous silicon dioxide is consistent with previous MD/DFT studies[48] where it is suggested that the most stable clusters adopt an equiaxed geometry, as observed for the copper tetramer shown in the inset of Figure 6 at t=4.0 ns.

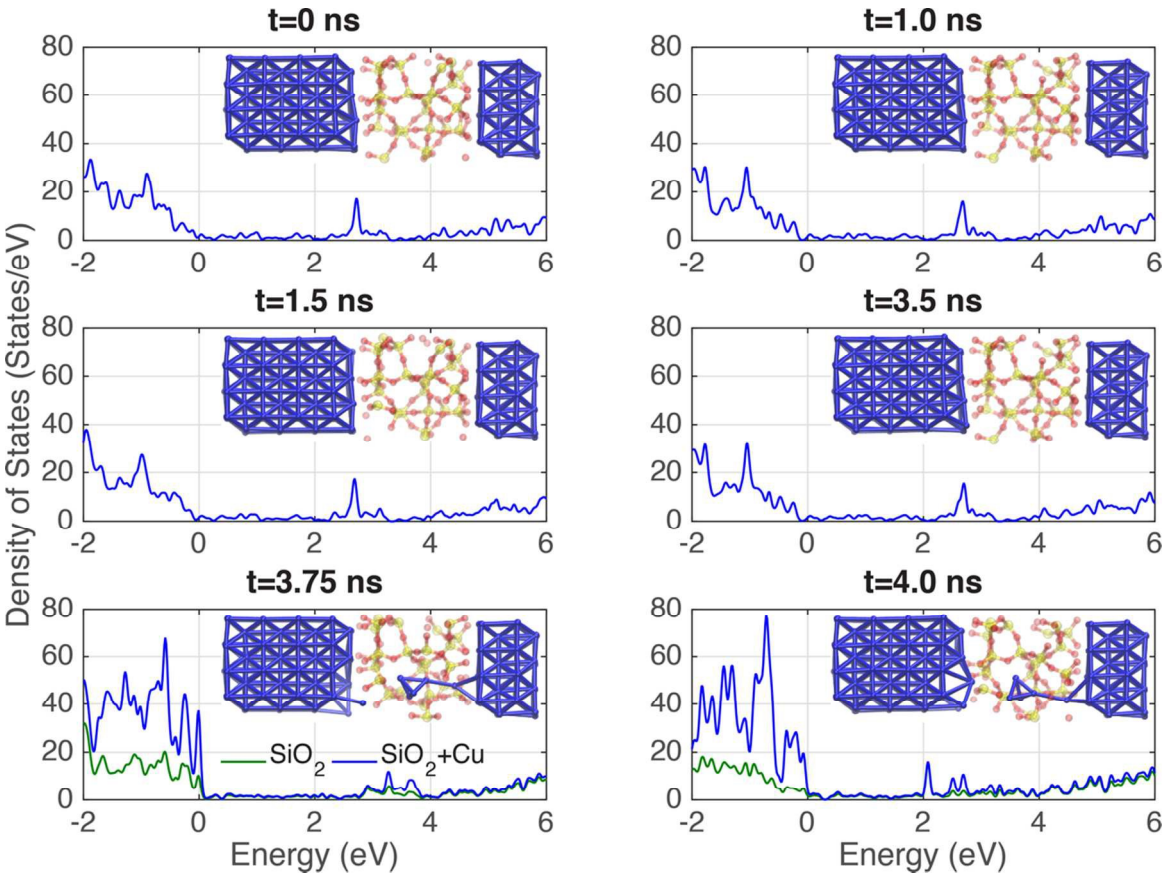

Figure 6. Projected density of states for small electrochemical metallization cell devices and snapshots of the atomic structure throughout the switching process. The density of states has been projected on the atoms of the solid electrolyte region

Figure 7 provides a measure of the change in electronic conductance of device during switching, we show the density of states integrated in a Fermi window of +/- 0.2 eV as function of simulation time. As described above, there is a sudden increase in the number of states around the Fermi level when copper ions are embedded in the silicon dioxide. The DFT calculation (blue circles) is compared with EChemDID electronic current obtained from Eq. 4. Both methods show very similar trends lending credence to the EChemDID current calculation as an accurate estimator. We note that these simulation cells are smaller than those described in Section 3, which would result in quantum confinement and other size effects that affect the predictions.

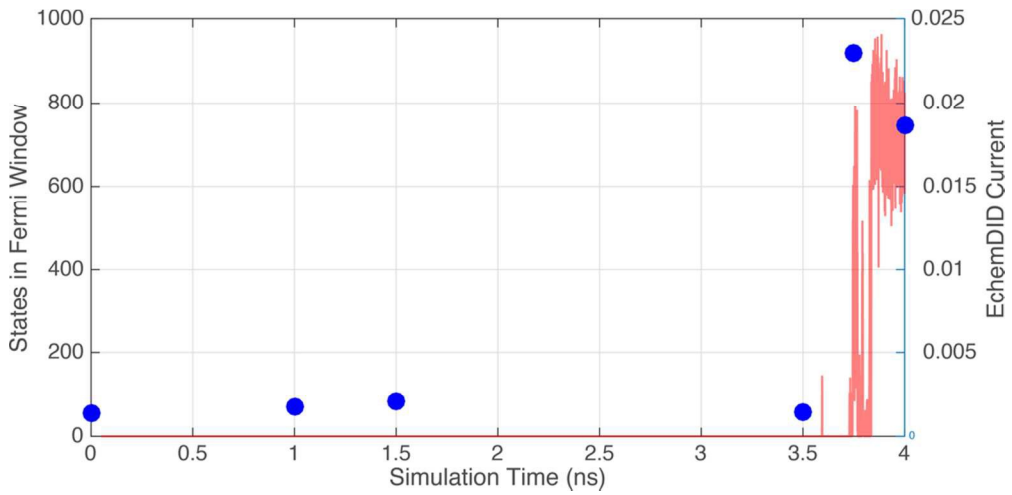

Figure 7. Integrated density of states in a Fermi window of +/- 0.2 eV. The variation of the number of states in the early stages of the simulation is associated to the continuously changing atomic structure of the amorphous silicon dioxide. The sudden increase in states available for conduction is attributed to the inclusion of copper ions in the solid electrolyte.

5. Conclusions and outlook

In summary this paper describes EChemDID, a model to perform large-scale reactive atomistic simulations of electrochemical processes, and its application to simulate resistive switching in nanoscale ECMs. MD simulations provide unparalleled resolution for devices at their scalability limit (nanometer dimensions) and at ultra-fast switching conditions of interest in many applications. The simulations, with no adjustable parameters, predict switching in nanosecond timescales and significant device to device variability, this is consistent with experimental observations. The simulations indicate that nanowire devices consisting of active electrode shells and where ions move in a convergent geometry towards the inactive electrode core switch at shorter timescale than those involving parallel electrodes. Given the significant device to device variability a larger number of simulations would be required to assess the distribution of performance (e.g. switching timescales, filaments stability) of the various devices. The simulations confirm that a threshold density of dissolved ions is necessary for switching (in the case of Cu/SiO_2 systems this value is 4% Cu per silica formula unit); but this condition is not sufficient. The formation of a stable filament required the formation is small Cu clusters that help the stability especially near the active electrode. Electrochemical reduction stabilizes thin filaments near the inactive electrode leading to filaments thinner near the negative electrode.

A detailed characterization of the atomic structure of the dielectric during switching shows no indication of the disruption of the amorphous network during the dissolution of the ions and the formation of a nanoscale conductive bridge. The amorphous network accommodates the ions with little distortions and this is confirmed by electronic structure calculations using

density functional theory that shows that during switching the electronic states near the Fermi energy responsible to conductance are predominantly associated with the Cu ions.

We stress that no model parameter was adjusted to describe ECMs or even electrochemistry; in that sense the models described in this paper are predictive. Of course, the simulations make several approximations that need to be taken into account when interpreting the results. The ReaxFF force field (as any other method to compute energies and interatomic forces, including most ab initio ones) provides an approximate description of the interactions. For example, the potential we use slightly underestimates the dissolution energy of Cu into SiO_2; the uncertainties introduced in the simulations due this effect have been discussed in detail in Ref. [10]. The atomic-based charge equilibration method used here has limitations that have been documented in recent papers[49,50]. Importantly for our specific application is that we neglect integer charge transfer processes (a dissolved ion or defect in the dielectric trapping a hole or electron); we consider the Cu ions to carry an *average* charge as they migrate through the dielectric. Müser and collaborators recently proposed an approach to capture such processes[51] and used to simulate a model battery.[52] Combining this approach with EChemDID would be worthwhile and its parameterization could be performed from first principles calculations.[46] Our simulations also neglect electric transport when a filament forms. Performing a detailed calculation of the possible Joule heating and electromigration on the nanoscale filaments predicted by EChemDID, accounting for possible ballistic effects on electron transport, would provide significant insight into their role in switching. This is particularly important to understand the dissolution of the filament during the RESET process and the current is externally limited during filament formation.

Finally we point out that EChemDID is quite generally applicable and could be used in conjunction with reactive force fields to simulate a wide range of devices including pseudo capacitors and batteries in addition to ECMs.

Acknowledgements

This work was supported by the FAME Center, one of six centers of STARnet, a Semiconductor Research Corporation program sponsored by MARCO and DARPA. Computational resources of nanoHUB.org and Purdue University are gratefully acknowledged.

6. References

[1] Dunn, Bruce, Haresh Kamath, and Jean-Marie Tarascon. "Electrical energy storage for the grid: a battery of choices." *Science* 334.6058 (2011): 928-935.

[2] Lu, Wei, and Charles M. Lieber. "Nanoelectronics from the bottom up." *Nature materials* 6, no. 11 (2007): 841-850.

[3] Waser, Rainer, and Masakazu Aono. "Nanoionics-based resistive switching memories." *Nature materials* 6, no. 11 (2007): 833-840.

[4] Borghetti, Julien, Gregory S. Snider, Philip J. Kuekes, J. Joshua Yang, Duncan R. Stewart, and R. Stanley Williams. "'Memristive'switches enable 'stateful'logic operations via material implication." *Nature* 464, no. 7290 (2010): 873-876.

[5] Valov, Ilia, et al. "Electrochemical metallization memories—fundamentals, applications, prospects." *Nanotechnology* 22.25 (2011): 254003.

[6] Jo, Sung Hyun, Ting Chang, Idongesit Ebong, Bhavitavya B. Bhadviya, Pinaki Mazumder, and Wei Lu. "Nanoscale memristor device as synapse in neuromorphic systems." *Nano letters* 10, no. 4 (2010): 1297-1301.

[7] Prezioso, Mirko, Farnood Merrikh-Bayat, B. D. Hoskins, G. C. Adam, Konstantin K. Likharev, and Dmitri B. Strukov. "Training and operation of an integrated neuromorphic network based on metal-oxide memristors." *Nature* 521, no. 7550 (2015): 61-64.

[8] Yang, Yu Chao, et al. "Fully room-temperature-fabricated nonvolatile resistive memory for ultrafast and high-density memory application." *Nano letters* 9.4 (2009): 1636-1643.

[9] Dapp WB, Müser MH. Redox reactions with empirical potentials: Atomistic battery discharge simulations. The Journal of chemical physics. 2013 Aug 14;139(6):064106.

[10] Onofrio N, Guzman D, Strachan A. Atomic origin of ultrafast resistance switching in nanoscale electrometallization cells. Nature materials. 2015 Apr 1;14(4):440-6.

[11] Onofrio N, Strachan A. Voltage equilibration for reactive atomistic simulations of electrochemical processes. The Journal of chemical physics. 2015 Aug 7;143(5):054109.

[12] Waser, Rainer, Regina Dittmann, Georgi Staikov, and Kristof Szot. "Redox-based resistive switching memories–nanoionic mechanisms, prospects, and challenges." *Advanced Materials* 21 (2009): 2632-2663.

[13] Yang, J. Joshua, Dmitri B. Strukov, and Duncan R. Stewart. "Memristive devices for computing." *Nature nanotechnology* 8, no. 1 (2013): 13-24.

[14] Padilla, Alvaro, Burr, G.W. ; Shenoy, R.S. ; Raman, K.V. ; Bethune, D.S. ; Shelby, R.M. ; Rettner, C.T. ; Mohammad, J. ; Virwani, K. ; Narayanan, P. ; Deb, A.K. ; Pandey, R.K. ; Bajaj, M. ; Murali, K.V.R.M. ; Kurdi, B.N. ; Gopalakrishnan, K. "On the Origin of Steep–Nonlinearity in Mixed-Ionic-Electronic-Conduction-Based Access Devices." *Electron Devices, IEEE Transactions on* 62, no. 3 (2015): 963-971.

[15] Zhirnov, Victor V., Roy Meade, Ralph K. Cavin, and Gurtej Sandhu. "Scaling limits of resistive memories." *Nanotechnology* 22, no. 25 (2011): 254027.

[16] Yang, Yuchao, Peng Gao, Siddharth Gaba, Ting Chang, Xiaoqing Pan, and Wei Lu. "Observation of conducting filament growth in nanoscale resistive memories." *Nature communications* 3 (2012): 732.

[17] Valov, Ilia, Ina Sapezanskaia, Alpana Nayak, Tohru Tsuruoka, Thomas Bredow, Tsuyoshi Hasegawa, Georgi Staikov, Masakazu Aono, and Rainer Waser. "Atomically controlled electrochemical nucleation at superionic solid electrolyte surfaces." *Nature materials* 11, no. 6 (2012): 530-535.

[18] Wedig, Anja, Michael Luebben, Deok-Yong Cho, Marco Moors, Katharina Skaja, Vikas Rana, Tsuyoshi Hasegawa, Kiran K. Adepalli, Bilge Yildiz, Rainer Waser and Ilia Valov. "Nanoscale cation motion in TaOx, HfOx and TiOx memristive systems." *Nature nanotechnology* (2015).

[19] Stillinger, Frank H., and Thomas A. Weber. "Computer simulation of local order in condensed phases of silicon." *Physical review B* 31.8 (1985): 5262.

[20] Tersoff, J. "Modeling solid-state chemistry: Interatomic potentials for multicomponent systems." *Physical Review B* 39.8 (1989): 5566.

[21] Rappe, Anthony K., and William A. Goddard III. "Charge equilibration for molecular dynamics simulations." *The Journal of Physical Chemistry* 95, no. 8 (1991): 3358-3363.

[22] Mortier, Wilfried J., Swapan K. Ghosh, and S. Shankar. "Electronegativity-equalization method for the calculation of atomic charges in molecules." *Journal of the American Chemical Society* 108, no. 15 (1986): 4315-4320.

[23] Van Duin, Adri CT, et al. "ReaxFF: a reactive force field for hydrocarbons." *The Journal of Physical Chemistry A* 105.41 (2001): 9396-9409.

[24] Rick, Steven W., Steven J. Stuart, and Bruce J. Berne. "Dynamical fluctuating charge force fields: Application to liquid water." *The Journal of chemical physics* 101.7 (1994): 6141-6156.

[25] Stuart, Steven J., Alan B. Tutein, and Judith A. Harrison. "A reactive potential for hydrocarbons with intermolecular interactions." *The Journal of chemical physics* 112.14 (2000): 6472-6486.

[26] Wood MA, Cherukara MJ, Kober EM, Strachan A. Ultrafast Chemistry under Nonequilibrium Conditions and the Shock to Deflagration Transition at the Nanoscale. The Journal of Physical Chemistry C. 2015 Sep 11;119(38):22008-15.

[27] Castro-Marcano F, Kamat AM, Russo MF, van Duin AC, Mathews JP. Combustion of an Illinois No. 6 coal char simulated using an atomistic char representation and the ReaxFF reactive force field. Combustion and Flame. 2012 Mar 31;159(3):1272-85.

[28] Manzano H, Moeini S, Marinelli F, Van Duin AC, Ulm FJ, Pellenq RJ. Confined water dissociation in microporous defective silicates: mechanism, dipole distribution, and impact on substrate properties. Journal of the American Chemical Society. 2012 Jan 20;134(4):2208-15.

[29] Paupitz R, Autreto PA, Legoas SB, Srinivasan SG, van Duin AC, Galvao DS. Graphene to fluorographene and fluorographane: a theoretical study. Nanotechnology. 2012 Dec 21;24(3):035706.

[30] Van Duin, Adri CT, et al. "ReaxFFSiO reactive force field for silicon and silicon oxide systems." *The Journal of Physical Chemistry A* 107.19 (2003): 3803-3811.

[31] van Duin, Adri CT, et al. "Development and validation of a ReaxFF reactive force field for Cu cation/water interactions and copper metal/metal oxide/metal hydroxide condensed phases." *The Journal of Physical Chemistry A* 114.35 (2010): 9507-9514.

[32] Strachan, Alejandro, and Brad Lee Holian. "Energy exchange between mesoparticles and their internal degrees of freedom." *Physical review letters* 94.1 (2005): 014301.

[33] Lin, Keng-Hua, Brad Lee Holian, Timothy C. Germann, and Alejandro Strachan. "Mesodynamics with implicit degrees of freedom." *The Journal of chemical physics* 141, no. 6 (2014): 064107.

[34] Lin, Keng-Hua, and Alejandro Strachan. "Role of direct electron-phonon coupling across metal-semiconductor interfaces in thermal transport via molecular dynamics." *The Journal of chemical physics* 143, no. 3 (2015): 034703.

[35] Plimpton, Steve. "Fast parallel algorithms for short-range molecular dynamics." *Journal of computational physics* 117, no. 1 (1995): 1-19.

[36] https://nanohub.org/groups/strachangroup/lammpsmodules. Last visited Nov. 1.

[37] Valov, Ilia, and Michael N. Kozicki. "Cation-based resistance change memory." *Journal of Physics D: Applied Physics* 46.7 (2013): 074005.

[38] Bernard, Y., et al. "Back-end-of-line compatible conductive bridging RAM based on Cu and SiO 2." *Microelectronic Engineering* 88.5 (2011): 814-816.

[39] Menzel, Stephan, Ulrich Böttger, and Rainer Waser. "Simulation of multilevel switching in electrochemical metallization memory cells." *Journal of applied physics* 111.1 (2012): 014501.

[40] Kresse, Georg, and Jürgen Furthmüller. "Efficiency of ab-initio total energy calculations for metals and semiconductors using a plane-wave basis set." *Computational Materials Science* 6.1 (1996): 15-50.

[41] Kresse, Georg, and Jürgen Furthmüller. "Efficient iterative schemes for ab initio total-energy calculations using a plane-wave basis set." *Physical Review B* 54.16 (1996): 11169.

[42] Kresse, Georg, and D. Joubert. "From ultrasoft pseudopotentials to the projector augmented-wave method." *Physical Review B* 59.3 (1999): 1758.

[43] Perdew, John P., Kieron Burke, and Matthias Ernzerhof. "Generalized gradient approximation made simple." *Physical review letters* 77.18 (1996): 3865.

[44] Tsuruoka, Tohru, et al. "Effects of Moisture on the Switching Characteristics of Oxide-Based, Gapless-Type Atomic Switches." *Advanced Functional Materials* 22.1 (2012): 70-77.

[45] Anderson NL, Vedula RP, Schultz PA, Van Ginhoven RM, Strachan A. First-principles investigation of low energy E' center precursors in amorphous silica. Physical review letters. 2011 May 17;106(20):206402.

[46] Anderson, Nathan L., et al. "Defect level distributions and atomic relaxations induced by charge trapping in amorphous silica." *Applied Physics Letters* 100.17 (2012): 172908.

[47] Pandey, Sumeet C., Roy Meade, and Gurtej S. Sandhu. "Cu impurity in insulators and in metal-insulator-metal structures: Implications for resistance-switching random access memories." *Journal of Applied Physics* 117.5 (2015): 054504.

[48] Guzman, David M., Nicolas Onofrio, and Alejandro Strachan. "Stability and migration of small copper clusters in amorphous dielectrics." *Journal of Applied Physics* 117.19 (2015): 195702.

[49] Nistor, Razvan A., et al. "A generalization of the charge equilibration method for nonmetallic materials." *The Journal of chemical physics* 125.9 (2006): 094108.

[50] Verstraelen, Toon, et al. "ACKS2: Atom-condensed Kohn-Sham DFT approximated to second order." *The Journal of chemical physics* 138.7 (2013): 074108.

[51] Dapp, Wolf B., and Martin H. Müser. "Towards time-dependent, non-equilibrium charge-transfer force fields." *The European Physical Journal B* 86.7 (2013): 1-11.

[52] Dapp, Wolf B., and Martin H. Müser. "Redox reactions with empirical potentials: Atomistic battery discharge simulations." *The Journal of chemical physics* 139.6 (2013): 064106.